Applied Radiation and Isotopes 202 (2023) 111068

Contents lists available at ScienceDirect

Applied Radiation and Isotopes

journal homepage: www.elsevier.com/locate/apradiso

Comparison of calibration coefficients for a vinten ionization chamber simulated using four Monte Carlo methods

Brittany A. Broder *, Denis E. Bergeron, Ryan Fitzgerald, Brian E. Zimmerman

Physical Measurement Laboratory, National Institute of Standards and Technology, Gaithersburg, MD, 20899-8462, USA

ARTICLE INFO

Keywords:
Ionization chamber
Monte Carlo
Radionuclide calibrator
Secondary standard

ABSTRACT

The Vinten 671 ionization chamber (VIC) was modelled using Monte Carlo (MC) programs EGSnrc, Penelope, and TOPAS. Several national measurement institutes have VICs with well-characterized response relationships and have measured calibration coefficients for many radionuclides. Twelve radionuclides with various decay emissions were assessed as well as 14 monoenergetic photon sources and 10 monoenergetic electron sources. Calibration coefficients were calculated based on the energy deposited in the simulated VIC nitrogen gas volume and compared to experimental values from the literature.

1. Introduction

Re-entrant, well-type pressurized ionization chambers are devices in which the incident ionizing radiation from a radioactive source placed in the well produces ion pairs in the fill gas. The electrons migrate to the anode under an electric field, creating an electric current. For a given photon energy, the current is proportional to the incident radiation flux (Knoll, 2010). Ionization chambers are thus a valuable tool in radionuclide metrology, where the electrical current can be related to an activity and serve as a secondary standard.

Monte Carlo (MC) simulations are a useful tool in benchmarking a range of calibration devices, from confirming ionization chamber calibration coefficients to aiding the development of novel calibration systems. They can also be used to predict the response of a certain chamber to a radionuclide, providing a comparison that can guide experiments. A multitude of MC programs exist for various applications and are more tuned towards different user populations. While the underlying principles of MC programs are the same, they may differ in their physics and transport mechanisms. Modelling a similar geometry in various MC programs can increase confidence in the results and increase their utility. Additionally, MC models can be used as a tool for a near-primary measurement based on decay data and associated primary measurements (NCRP report 58).

Here, the Vinten 671 ionization chamber (VIC) was modelled. The VIC was designed to have traceability to radioactivity standards; to have a response independent of ambient pressure and temperature variations; and for the individual ionization chambers to have the same calibration figures for various nuclides within an uncertainty (Woods et al., 1983). VICs with well-characterized response relationships are deployed at several National Measurement Institutes (NMIs). Due to their utility and consistency among NMIs, they have been previously modelled using MC methods (Salvat et al., 2008; Townson et al., 2018).

In this study, modelling was conducted using three MC programs: EGSnrc (Kawrakow et al., 2000), Penelope (Salvat et al., 2008), and TOPAS (Perl et al., 2012). Additionally, two libraries were used to implement two EGSnrc models: egs_chamber and DOSRZnrc. Each of these MC programs is open source and publicly available, making any developed models easily transferrable between users. Each program has geometry and physics components that can be applicable for the types of radiation and geometries used to construct and test an ionization chamber. Over the course of more than 10 years, four VIC models were developed independently at the National Institute of Standards and Technology (NIST); here we assess differences among them. Each model was assessed by comparing monoenergetic photon and electron response curves and calibration coefficients for various nuclides spanning a variety of energies and emission types.

Calibration coefficients for many radionuclides have been measured, modelled, and compared between institutes. These experimental values are compared to the generated MC values in this work.

2. Methods

The Vinten 671 ionization chamber (VIC) has previously been described (Woods et al., 1983). It consists of sealed, concentric cylinders

* Corresponding author.
E-mail address: brittany.broder@nist.gov (B.A. Broder).

https://doi.org/10.1016/j.apradiso.2023.111068
Received 2 June 2023; Received in revised form 24 August 2023; Accepted 6 October 2023
Available online 17 October 2023
0969-8043/Published by Elsevier Ltd.

and an electrode surrounded by nitrogen gas. The chamber is described as having a gas pressure of 1 MPa.

Models of the VIC were developed based on drawings derived from computed tomography (CT) scans acquired at NIST, machine drawings, and parameters provided in the literature (Townson et al., 2018). Four Monte Carlo programs were used to conduct simulations: EGSnrc (egs_chamber) (2021 release, egs_chamber library), EGSnrc (DOSRZnrc) (2015 release, DOSRZnrc library), PENELOPE (2014 release), and TOPAS (version 3.8, 2022 release). Parameters of the simulations for each program are outlined in the MC methods table, Table 1.

Cross sectional views of the models developed in all four programs are shown in Fig. 1. Some quantitative parameters of the models are provided in Table 2. These parameters were chosen because they were used to adjust the models or are notably different between the models.

2.1. Model development

2.1.1. EGSnrc (egs_chamber) model development

Materials were defined using PEGS4 with user-defined densities. Electron/photon transport parameters included default Compton cross sections, bound Compton scattering, Raleigh scattering, and global cutoff energies of 521 keV for electrons and 10 keV for photons. The egs_radionuclide_source library was used to define the emissions from the liquid region in the ampoule. Decay data were read from evaluated nuclear structure data files (ENSDF; Bhat, 1992) downloaded from the decay data evaluation project (Decay Data). Dose scoring to defined media was enabled, so that the dose to the nitrogen fill gas could be used to calculate the VIC response in terms of pA/MBq as described in Section 2.2.1. The egs_chamber user code was used to run the simulations.

The geometry was designed using the egs_cones library (Kawrakow et al., 2000), with dimensions based on an x-ray computed tomography (CT) scan, the drawings given by Townson et al. (2018), and with reference to the dimensions used in the EGSnrc (DOSRZnrc) model described in Section 2.1.2. The dimensions of the ampoule were taken from Colle (2019). The chamber wall thickness and fill gas pressure were based on the values in Townson et al. (2018), but were adjusted to improve agreement with experiment and other models. The entire chamber was placed inside a large box (defined with egs_box) of air; the NIST VIC is operated without lead shielding, but scattering from surrounding walls and cabinetry is not accounted in this model.

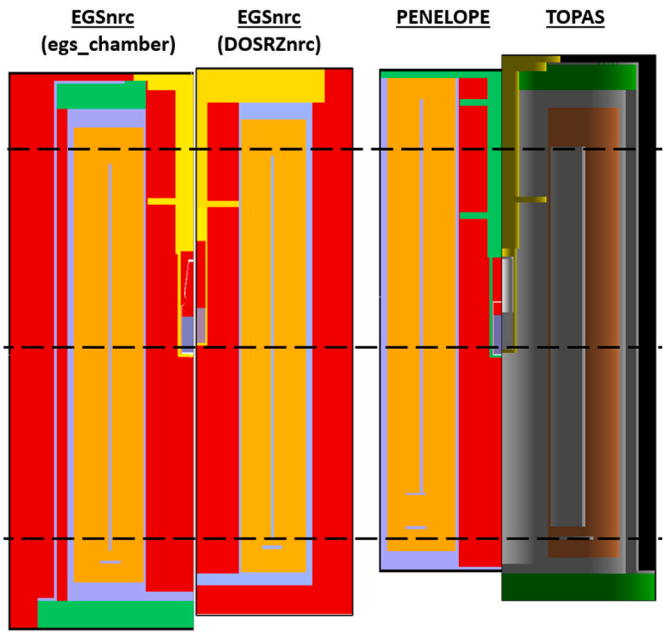

Fig. 1. Cross sectional views of models developed in MC programs. From the left, models in: EGSnrc (egs_chamber), EGSnrc (DOSRZnrc), PENELOPE, and TOPAS. The colors denote the different materials: red is air, orange is N_2 gas, yellow is polypropylene, grey is aluminum, dark grey is water, green is polymethyl methacrylate, and white is borosilicate glass. The dashed lines are shown for geographic comparison between models, with lines denoting (from the top): top of the long electrode; source volume; and bottom electrode. (For interpretation of the references to colour in this figure legend, the reader is referred to the web version of this article.)

2.1.2. EGSnrc (DOSRZnrc) model development

As with the EGSnrc (egs_chamber) model, materials were defined using PEGS4 with user-defined densities. Electron/photon transport parameters included default Compton cross sections, bound Compton

Table 1
Monte Carlo methods table. Included are parameters specific to the Monte Carlo programs used, including the version; literature reference in which the program is validated to attest to the legitimacy of its results; a description of the simulated source definition; the source of any physical or decay quantities used in the simulations; the transport parameters used; the quantity that was scored in order to obtain information that could be interpreted as a k-value; and the number of histories and methods to obtain statistical uncertainty.

	Program			
Parameter	EGSnrc (egs_chamber)	EGSnrc (DOSRZnrc)	PENELOPE	TOPAS
Version	Version 4, 2021 release	2015	2014	3.8, 2022 release
Validation	Bouchard et al. (2011), Townson et al. (2018)	Ali and Rogers (2008), Lee et al. (2018)	De Vismes and Amiot (2003)	Perl et al. (2012)
Timing	24–36 h/10^7 photons of 100 keV	100 s/10^7 photons of 100 keV	700 s/10^7 photons of 100 keV	135 s/10^7 photons of 100 keV
Source description	Volumetric; each point randomly selected	Volumetric; each point randomly selected	Volumetric, isototropic, each point randomly selected	Volumetric, sampled over 10^7 points
Source of derived quantities	EGSnrc, PEGS4, DDEP, ENSDF	EGSnrc, PEGS4, DDEP, ENSDF	PENDBASE, DDEP, ENSDF, BETASHAPE	TENDL, Geant4, ENSDF, DDEP
Transport Parameters	Electron (photon) transport cutoff 0.514 MeV (0.010 MeV); Bound Compton ON, Radiative Compton OFF, Raleigh ON; Atomic relaxations EADL	Electron (photon) transport cutoff 0.514 MeV (0.010 MeV); Bound Compton ON, Radiative Compton OFF, Raleigh ON; Atomic relaxations EADL	Global cutoff 1 keV for all parameters; all scattering, relaxation effects ON; maximum fractional energy loss 0.1; maximum cutoff energy of 5 keV for bremsstrahlung and hard collisions	Default to TOPAS
Scored Quantity	Energy deposited in nitrogen medium	Energy deposited	Energy deposited; summed across 29 defined regions	Energy deposited
# Histories, Statistical Uncertainty	10^7 to 10^8 decays or photon histories; statistical uncertainty from EGSnrc	10^7 histories per photon energy; statistical uncertainty from EGSnrc	10^7 (photons), 10^8 (electrons) histories; statistical; uncertainty from Penelope propagated through sum of all calculated regions	10^8 histories; standard deviation between batches; TOPAS statistical uncertainty

Table 2
Select parameters of the developed VIC models. The measured source height, defined as the distance from the top of the chamber to the bottom of the ampoule, was 21.6 cm.

Parameter	Program			
	EGSnrc (egs_chamber)	**EGSnrc (DOSRZnrc)**	**PENELOPE**	**TOPAS**
Source Height [cm]	21.01	21.24	21.86	21.19
Source Volume [cm^3]	4.93	4.93	5.96	5.00
N_2 Gas Volume [cm^3]	7258	7282	7340	7333
N_2 Gas Pressure [MPa]	1.068	1.072	1.098	1.072
Inner Aluminum Wall Thickness [cm]	0.22	0.19	0.23	0.18
Ion Chamber Length [cm]	36.4	36.0	38.3	37.14
Electrode Length [cm]	29.6	29.6	30.5	29.8
# Histories	10^7	10^7	10^7–10^9	10^8

scattering, Raleigh scattering, and global cutoff energies of 514 keV for electrons and 10 keV for photons. The radioactive source material was simulated as water. To simulate a radionuclide, the response for all γ-rays and X-rays and β particles produced in the decay were summed.

The user code DOSRZnrc was used to define a cylindrical geometry based on Townson et al. (2018) and CT scans. The model was run for 231 different photon energies between 12 keV and 4.02 MeV to generate a response curve. Additionally, the model was run for various beta spectra and the response tabulated as a function of beta endpoint energy. The gas pressure and inner wall thickness were then adjusted so that the generated response curve matched the experimental calibration coefficients for low and high energy gamma-ray emitters.

2.1.3. PENELOPE model development

Materials were defined using PENDBASE and the MATERIALS code using the default densities and other parameters as defined in the database files, with the exception of the nitrogen filling gas. Simulations for electrons and photons were followed from their initial energy to a global cutoff of 1 keV (including Compton and Rayleigh scattering). Initial energies were defined as originating from monoenergetic sources to develop the energy-response curves. Simulations of radionuclides were performed by calculating via separate simulations the response for all photons having an intensity of >1.0 per decay and summed with weighting by the respective emission probabilities. The electron responses for beta emitters were calculated for each nuclide using the summed spectrum from BETASHAPE (Mougeot, 2017). The resulting electron response value was summed with the photon response (with appropriate weighting for total beta emission probability) to arrive at a combined response value per decay for the nuclide.

The model was originally developed to perform simulations over a range of 50 keV–1200 keV, which covered most nuclides of interest at that time. For that reason, the gas density and pressure were adjusted to fit the calculated energy-response curve to available experimental data for photons between 50 keV and 1.5 MeV. The geometry was defined for the PENCYL user code using the original design drawings, which were confirmed to within 0.675 mm using a CT image of the chamber maintained at NIST. Definitions for the source holder were taken from a separate set of design drawings. The source holder used in this study was not included in the CT scan.

2.1.4. TOPAS model development

Materials were defined based on parameters including their constituent atom fraction, density, state, temperature, and pressure to reflect those described in the EGSnrc (egs_chamber) and EGSnrc (DOSRZnrc) models. TOPAS is a Geant4-based program and consequently imposes range production thresholds as opposed to energy cuts; this was defined to be 0.05 mm for all particles. The radioactive source is defined as a 'volumetric' distribution of the nuclide within a water volume in the ampoule. Decay properties of nuclide sources are based on parameter files in TOPAS that draw from DDEP and ENSDF data. Default physics parameters were used with the addition of the 'g4radioactivedecay' module to enable radioactive decay.

Model dimensions were determined based on the above EGSnrc (egs_chamber) model, CT drawings, and measurements of the VIC at NIST. After the initial model construction, the chamber measurements were adjusted primarily in terms of the thickness of the inner wall of the cylinder containing the nitrogen volume and the pressure of the N_2 gas contained within the volume. These parameters were optimized to best fit the experimental calibration coefficients of a subset of nuclides.

2.2. Model evaluation

2.2.1. Evaluating calibration coefficients

In each simulation program, the energy deposited in the nitrogen gas volume was assessed. This metric was then converted to a calibration coefficient, k. The calibration coefficient is a factor relating the chamber current, I, in pA to the activity, A, in MBq of a radionuclide:

$$k_{\mathrm{exp}} = \frac{I}{A} \tag{1}$$

Similarly, k can also be calculated for MC simulations, where the number of decays, N, is known:

$$k_{\mathrm{MC}} = \frac{I}{A} = \frac{Q}{N} = e\frac{\left(\frac{E}{N}\right)}{W} \tag{2}$$

Where W is the average energy to create a single ion-pair in nitrogen (W = 34.8(2) eV) assuming complete charge collection, e is the elementary charge (e = 1.602 10^{-19} C), and E is the energy deposited in the nitrogen gas volume.

2.2.2. Comparison metrics

Each model was evaluated based on a subset of nuclides, chosen to reflect a variety of decay emission properties. These nuclides include fluorine-18, sodium-22, copper-64, germanium-68, yttrium-90, technetium-99 m, indium-111, iodine-123, iodine-125, barium-133, lutetium-177, and lead-212. Where possible, the resulting calibration coefficients were compared to NIST standards (Bergeron and Cessna, 2018; Bergeron et al., 2022); otherwise, values were compared to those provided by Townson et al. (2018). The relative difference between the MC calibration coefficient and the experimental calibration coefficient was calculated for each nuclide according to Equation (3). The root mean square was taken over all deviations (d_{rms}) according to Equation (4) and served as a metric of comparison.

$$d_i = \frac{k_{MC}}{k_{Exp}} - 1 \tag{3}$$

$$d_{rms} = \sqrt{\frac{1}{N}\sum_i d_i^2} \tag{4}$$

Additionally, monoenergetic photon and electron sources were simulated to produce respective response curves. Included in the response curves were 34 photon energies from 12 keV to 4.02 MeV and 10 electron energies from 0.2 MeV to 2.0 MeV. The model with the smallest difference compared to response curves in the literature was chosen to study how chamber response is affected by the thickness of the inner wall of the chamber; the pressure of the nitrogen gas volume; and the source height, defined as the distance from the top of the chamber to

the bottom of the ampoule. The two former parameters (wall thickness, gas pressure) are of interest because they are not exactly known for an individual VIC and are difficult to measure experimentally. The latter parameter (source height) is of interest due to its sensitivity in the clinical assays of radiopharmaceuticals.

3. Results

3.1. Nuclide sources

The calibration coefficients were assessed for the 12 nuclides, reported in Section 2.2.2, spanning a variety of decay particle types and emission energies. The results, normalized to the associated experimental calibration coefficient in the literature (Bergeron and Cessna, 2018; Townson et al., 2018; Bergeron et al., 2022), are shown in Fig. 2. The k-value of each nuclide and the associated uncertainty is provided in Table 1S in the supplementary information. Overall, 89 % of MC calibration coefficients agreed within 5 % of the reported experimental value; 82 % of values agreed within 2 %, and 50 % of values agreed within 1 %. The d_{rms} was calculated over all nuclides for each program used; the value was 4.77 % for EGSnrc (egs_chamber), 0.96 % for EGSnrc (DOSRZnrc), 15.73 % for PENELOPE, and 0.84 % for TOPAS.

The largest deviation was in the calibration coefficient for ^{125}I, likely due to its low energy and Auger electrons. The emission intensities specified in the decay data could also contribute to this difference; decay data comes from either ENSDF or DDEP depending on the information available. The PENELOPE model had a particularly low k-value. It had both the largest inner aluminum wall thickness and the largest source volume; combined, these geometric effects could have contributed to the lower k-value. ^{212}Pb also somewhat deviated from the experimental calibration coefficient, perhaps due to its progeny. The contribution of four nuclides to the overall calibration coefficient, rather than just 1, provides additional sources of error. Overall, ^{212}Pb contributes 9.4 % of the calibration coefficient; ^{212}Bi 8.9 %; ^{211}Po 0.1 %; and ^{208}Tl 81.6 %. The calibration coefficient is therefore sensitive to the half-lives and branching ratio used to calculate the Bateman coefficients; any improvements to these decay data could potentially improve agreement with experimental values.

3.2. Monoenergetic sources

Of the models, the TOPAS model agreed best with experimental values in the literature, reflected as the smallest d_{rms}. Therefore, the TOPAS model was chosen for comparison and to further examine the effect of model variations on calibration coefficient output.

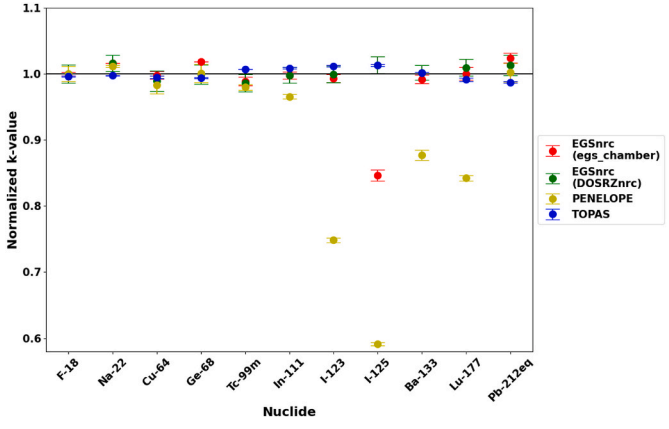

Fig. 2. Calibration coefficient per nuclide, normalized to the associated experimental calibration coefficient in the literature (Bergeron and Cessna, 2018; Townson et al., 2018; Bergeron et al., 2022). 89 % of MC calibration coefficients agreed within 5 % of the reported experimental value; 82 % of values agreed within 2 %, and 50 % of values agreed within 1 %.

3.2.1. Monoenergetic photon sources

Monoenergetic photons ranging from 12 keV to 4.02 MeV were placed in the source volume. Fig. 3A shows the resulting response curve. The photon response curve from Townson et al. (2018) is provided where values were available for comparison. Compared to the Townson et al. (2018) values across all photon sources, the d_{rms} was 5.71 % for EGSnrc (egs_chamber), 3.02 % for EGSnrc (DOSRZnrc), 4.69 % for PENELOPE, and 2.91 % for TOPAS.

Fig. 4A shows the ratio between the k_{MC} value for each program and the k_{MC} value for the TOPAS model for monenergetic photon sources. The greatest differences are at the lowest energy, with EGSnrc (egs_chamber) and PENELOPE having >25 % difference below 20 keV. Overall, the programs agreed fairly well for most energies: 91 % of EGSnrc (egs_chamber) values, 79 % of EGSnrc (DOSRZnrc) values, and 85 % of PENELOPE values agreed with TOPAS values within 5 %.

3.2.2. Monoenergetic electron sources

Monoenergetic electrons ranging from 0.2 MeV to 2.0 MeV were placed in the source volume. Fig. 3B shows the resulting response curve. Fig. 4B shows the ratio between the k_{MC} value for each program and the k_{MC} value for the TOPAS model for monenergetic electron sources. The greatest differences are at higher energy, with agreement being poor above 1.6 MeV for all models; this can perhaps be attributed to differences in transport parameters and in nominal gas pressure of the fill gas volume.

3.3. Variation in key parameters

As shown in Fig. 1 and Table 2, the models varied across several different parameters. Three parameters were identified as potentially impacting the resulting calibration coefficient: the thickness of the inner aluminum, through which any emissions would have to traverse when going from the source to the N_2 volume; the pressure of the N_2 gas, in which the energy deposited was scored to calculate the calibration coefficient; and the height of the source, which could impact geometry efficiency, or the fraction of the N_2 volume that could be irradiated by the source. Fig. 5 shows the variation from changing these parameters when assessing calibration coefficient for monoenergetic photons in the TOPAS model. The nominal simulation parameters were a 0.19 cm inner wall thickness, 1.072 MPa N_2 gas pressure, and 0 cm source height variation, corresponding to a source 19.67 cm from the top of the chamber to the middle of the source. The measured source height was 21.6 cm.

Fig. 5A shows that as wall thickness decreased, the calibration coefficient increased at all energies. The wall thickness had greater impact on calibration coefficient variation at lower energies: the calibration coefficient varied more than 5 % for all wall thicknesses below 60 keV. Less than 1 % variation was seen for energies above 1 MeV.

The decrease in calibration coefficient with increasing wall thickness is due to the photon transmission at this inner wall surface. Smaller thicknesses allow more photons to pass through into the gas volume, particularly for low energy photons.

Fig. 5B shows that as gas pressure decreased, calibration coefficient decreased at all energies. Different gas pressure resulted in larger variation in calibration coefficient at low energies, particularly for 1.0 MPa, (the lowest pressure assessed) which had greater than 5 % variation at all energies. Above 1 MeV, the variation was stable per gas pressure at an average of 6.09 % for 1.0 MPa, 0.85 % for 1.062 MPa, 0.41 % for 1.067 MPa, and 2.37 % for 1.1 MPa.

The decrease in calibration coefficient with decreasing gas pressure is due to the photons interacting in the gas volume: as the pressure increases, the photons are more likely to interact with a gas particle and are more likely to deposit energy in the volume.

Fig. 5C shows that as source height changes away from the initial

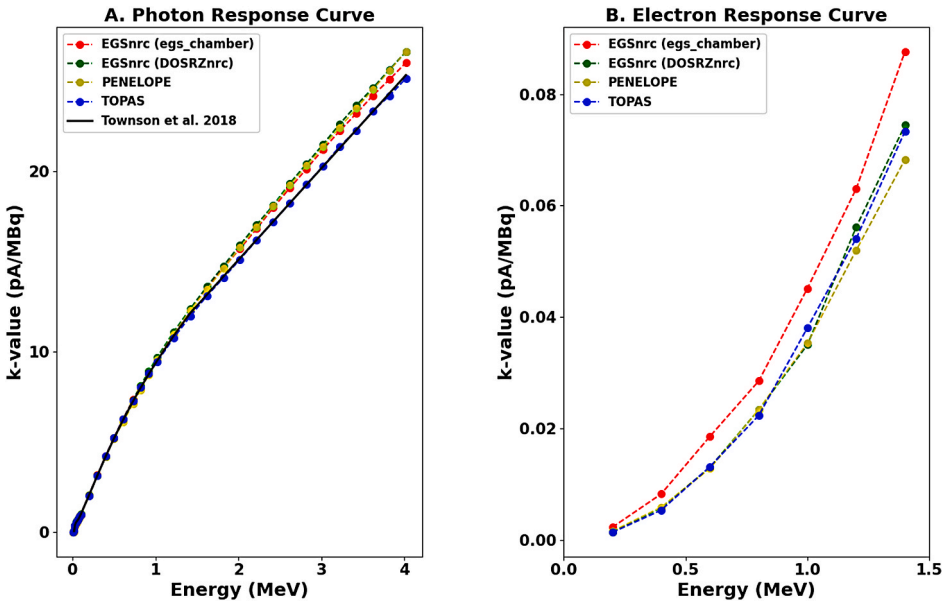

Fig. 3. Response curves for monoenergetic photon (left, Fig. 3A) and select monoenergetic electron (right, Fig. 3B) sources. Data from a simulated photon response curve in Townson et al. (2018) is provided for comparison.

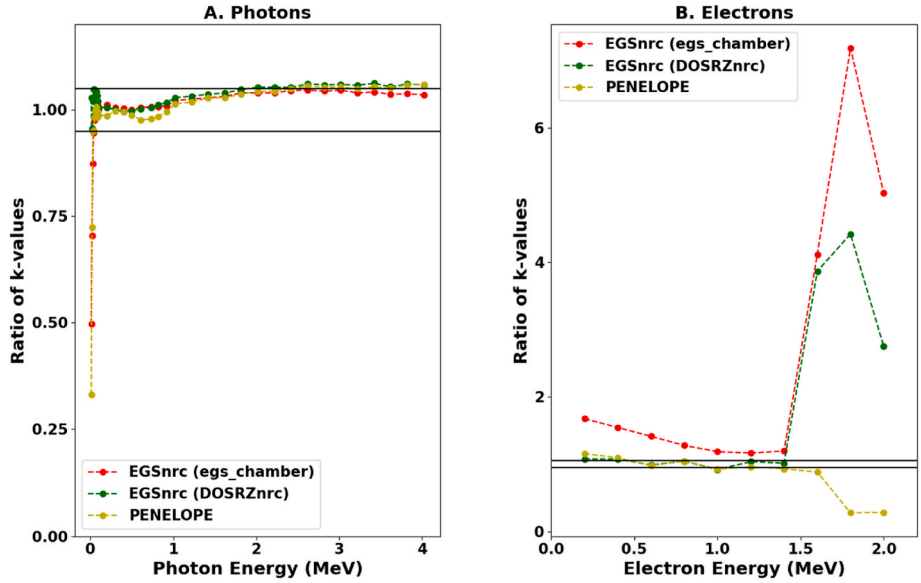

Fig. 4. Ratio of the calibration coefficient for various MC programs compared to TOPAS. The black lines mark a 5% difference. The values are more similar for the photon sources compared to the electron sources: 59 % of EGSnrc (egs_chamber) values, 82 % of EGSnrc (DOSRZnrc) values, and 65 % of PENELOPE values agreed with TOPAS values within 5 %. For monoenergetic electron sources, less than 30 % of values agreed with the TOPAS data within 5 %.

source height, the calibration coefficient decreases, with the decrease being greater with greater displacement. Changing the source height resulted in a large variation in calibration coefficient at low energies. Above 1 MeV, varying the source height by 1 cm in either direction resulted in lower variation than varying the source height by 3 cm in either direction. The variation due to source height was less than the other factors: wall thickness changed the calibration coefficient by as much as 400 %, gas pressure changed the calibration coefficient by as much as 17 %, while source height changed the calibration coefficient by at most 2 %. The nominal source height was chosen to optimize the agreement between MC calibration coefficient and experimental values, resulting in decreasing calibration coefficient with deviation.

4. Discussion

While the models presented herein drew upon common information in their development, they were tested according to different criteria and have different geometric properties, as demonstrated in Table 2. These differences can change how the particles interact in the model. While four models may not be necessary to routinely model radionuclide sources, each model has its advantages. The EGSnrc (DOSRZnrc) model may be more equipped to model sources with a variety of emission properties, as demonstrated by its low d_{rms} in section 3.1. The TOPAS model can be used in a multithreaded environment, making it more suitable for simulations with large amounts of histories or those run on a computing cluster. Additionally, having all four models provides a metric of comparison to increase confidence in the result.

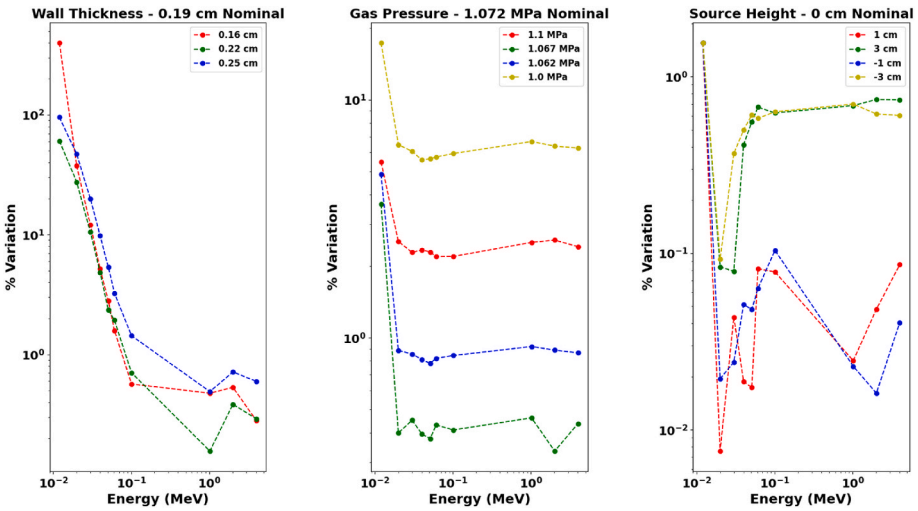

Fig. 5. Difference in calibration coefficient resulting from varying the thickness of the inner aluminum wall (Fig. 5A), varying the pressure of the N_2 gas in which energy is deposited (Fig. 5B), and moving the source relative to its origin (Fig. 5C). The nominal simulation parameters were a 0.19 cm inner wall thickness, 1.072 MPa N_2 gas pressure, and 0 cm variation, corresponding to a source 19.67 cm from the top of the chamber.

This ionization chamber is similar to radionuclide calibrators that are used in radiopharmacies and clinical nuclear medicine settings, indicating that these models could be adapted to further verify radionuclide calibrator settings and to predict how calibrator response may change with source geometry or chemical composition.

These models could become the basis of an uncertainty engine that builds on the uncertainty of activity assays. In addition to statistical uncertainties, simulations could provide uncertainties on attributes such as source volume, known decay data, and source height.

5. Conclusions

This work demonstrated the utility of four Monte Carlo programs in modelling the Vinten 671 ionization chamber, showing that VIC models are a valuable tool in predicting and validating experimental response values. By using updated decay data and associated primary measurements, VIC MC models can provide a near-primary measurements. Simulations can serve as confirmatory measurements in activity standardization campaigns by contributing a means of comparison for experimental values. Iterative simulations can also provide a check on photon emission intensities, with improved data providing better agreement.

Differences in calibration coefficients between models could be attributed to differences in geometry, validation methods, and program implementation of physics and decay properties. These factors are particularly important for low energy particles, resulting in the largest variation between calibration coefficients at low energies. Overall, the TOPAS model agrees best with both experimental radionuclide calibration coefficients and monoenergetic source values from the literature. The current PENELOPE model, which was not optimized for beta emitters or photons above 1.2 MeV, demonstrated good utility but requires additional refinement to perform to its full potential.

Future work could include adapting the VIC model to radionuclide calibrators used in clinical nuclear medicine settings to further verify calibration settings. These models could also provide the basis of an uncertainty engine to build on the uncertainty of activity assays by providing uncertainties on attributes such as source volume, known decay data, and source height in addition to statistical uncertainties.

Disclaimer: Certain commercial equipment, instruments, or materials are identified in this paper to foster understanding. Such identification does not imply recommendation by the National Institute of Standards and Technology, nor does it imply that the materials or equipment identified are necessarily the best available for the purpose.

CRediT authorship contribution statement

Brittany A. Broder: Writing – review & editing, Writing – original draft, Visualization, Formal analysis, Data curation. **Denis E. Bergeron:** Writing – review & editing, Methodology, Conceptualization. **Ryan Fitzgerald:** Writing – review & editing, Methodology, Investigation, Data curation. **Brian E. Zimmerman:** Writing – review & editing, Supervision, Investigation.

Declaration of competing interest

The authors declare that they have no known competing financial interests or personal relationships that could have appeared to influence the work reported in this paper.

Data availability

Data will be made available on request.

Appendix A. Supplementary data

Supplementary data to this article can be found online at https://doi.org/10.1016/j.apradiso.2023.111068.

References

Ali, E.S.M., Rogers, D.W.O., 2008. Benchmarking EGSnrc in the kilovoltage energy range against experimental measurements of charged particle backscatter coefficients. Phys. Med. Biol. 53 (6), 1527.

Bergeron, D.E., Cessna, J.T., 2018. An update on "dose calibrator" settings for nuclides used in nuclear medicine. Nucl. Med. Commun. 39 (6), 500.

Bergeron, D.E., Cessna, J.T., Fitzgerald, R.P., Laureano-Pérez, L., Pibida, L., Zimmerman, B.E., 2022. Primary standardization of 212Pb activity by liquid scintillation counting. Appl. Radiat. Isot. 190, 110473.

Bhat, M.R., 1992. Evaluated nuclear structure data file (ENSDF). In: Nuclear Data for Science and Technology: Proceedings of an International Conference, Held at the Forschungszentrum Jülich, Fed. Rep. Of Germany, 13–17 May 1991. Springer Berlin Heidelberg, pp. 817–821.

Bouchard, H., Seuntjens, J., Kawrakow, I., 2011. A Monte Carlo method to evaluate the impact of positioning errors on detector response and quality correction factors in nonstandard beams. Phys. Med. Biol. 56 (8), 2617.

Colle, R., 2019. Ampoules for Radioactivity Standard Reference Materials. US Department of Commerce, National Institute of Standards and Technology.

De Vismes, A., Amiot, M.N., 2003. Towards absolute activity measurements by ionisation chambers using the PENELOPE Monte-Carlo code. Appl. Radiat. Isot. 59 (4), 267–272.

Decay Data Evaluation Project, LNHB. Available: http://www.lnhb.fr/ddep_wg/.

Kawrakow, I., Rogers, D.W.O., Mainegra-Hing, E., Tessier, F., Townson, R.W., Walters, B. R.B., 2000. EGSnrc Toolkit Monte Carlo Simulation Ionizing Radiation Transp. https://doi.org/10.4224/40001303.

Knoll, G.F., 2010. Radiation Detection and Measurement. John Wiley & Sons.

Lee, J., Lee, J., Ryu, D., Lee, H., Ye, S.J., 2018. Fano cavity test for electron Monte Carlo transport algorithms in magnetic fields: comparison between EGSnrc, PENELOPE, MCNP6 and Geant4. Phys. Med. Biol. 63 (19), 195013.

Mougeot, X., 2017. BetaShape: a new code for improved analytical calculations of beta spectra. EPJ Web Conf. 146, 12015. EDP Sciences.

NCRP report 58, "A Handbook of Radioactivity Measurements Procedures.".

Perl, J., Shin, J., Schümann, J., Faddegon, B., Paganetti, H., 2012. TOPAS: an innovative proton Monte Carlo platform for research and clinical applications. Med. Phys. 39 (11), 6818–6837.

Salvat, F., Fernández-Varea, J. M., & Sempau, J. PENELOPE-2008: A Code System for Monte Carlo Simulation of Electron and Photon Transport..

Townson, R., Tessier, F., Galea, R., 2018. EGSnrc calculation of activity calibration factors for the Vinten ionization chamber. Appl. Radiat. Isot. 134, 100–104.

Woods, M.J., Callow, W.J., Christmas, P., 1983. The NPL radionuclide calibrator—type 271. Int. J. Nucl. Med. Biol. 10 (2–3), 127–132.